

3 MAGNETIC SHIELDING OF EXOMOONS BEYOND THE CIRCUMPLANETARY HABITABLE EDGE

4 RENÉ HELLER¹

5 McMaster University, Department of Physics and Astronomy, Hamilton, ON L8S 4M1, Canada; rheller@physics.mcmaster.ca

6 AND

7 JORGE I. ZULUAGA²

8 FACom - Instituto de Física - FCEN, Universidad de Antioquia, Calle 70 No. 52-21, Medellín, Colombia; jzuluaga@fisica.udea.edu.co

Draft version November 20, 2018

9 ABSTRACT

10 With most planets and planetary candidates detected in the stellar habitable zone (HZ) being super-
11 Earths and gas giants, rather than Earth-like planets, we naturally wonder if their moons could be
12 habitable. The first detection of such an exomoon has now become feasible, and due to observational
13 biases it will be at least twice as massive as Mars. But formation models predict moons can hardly
14 be as massive as Earth. Hence, a giant planet’s magnetosphere could be the only possibility for such
15 a moon to be shielded from cosmic and stellar high-energy radiation. Yet, the planetary radiation
16 belt could also have detrimental effects on exomoon habitability. We here synthesize models for the
17 evolution of the magnetic environment of giant planets with thresholds from the runaway greenhouse
18 (RG) effect to assess the habitability of exomoons. For modest eccentricities, we find that satellites
19 around Neptune-sized planets in the center of the HZ around K dwarf stars will either be in an RG
20 state and not be habitable, or they will be in wide orbits where they will not be affected by the
21 planetary magnetosphere. Saturn-like planets have stronger fields, and Jupiter-like planets could coat
22 close-in habitable moons soon after formation. Moons at distances between about 5 and 20 planetary
23 radii from a giant planet can be habitable from an illumination and tidal heating point of view, but
24 still the planetary magnetosphere would critically influence their habitability.

25 *Keywords:* astrobiology – celestial mechanics – methods: analytical – planets and satellites: magnetic
26 fields – planets and satellites: physical evolution – planet-star interactions

27 1. INTRODUCTION

28 The search for life on worlds outside the solar system
29 has experienced a substantial boost with the launch of
30 the *Kepler* space telescope in 2009 March (Borucki et al.
31 2010). Since then, thousands of planet candidates have
32 been detected (Batalha et al. 2013), several tens of which
33 could be terrestrial and have orbits that would allow for
34 liquid surface water (Kaltenegger & Sasselov 2011). The
35 concept used to describe this potential for liquid water,
36 which is tied to the search for life, is called the “habitable
37 zone” (HZ) (Kasting et al. 1993). Yet, most of the *Kepler*
38 candidates, as well as most of the planets in the HZ de-
39 tected by radial velocity measurements, are giant planets
40 and not Earth-like. This leads us to the question whether
41 these giants can host terrestrial exomoons, which may
42 serve as habitats (Reynolds et al. 1987; Williams et al.
43 1997).

44 Recent searches for exomoons in the *Kepler* data (Kip-
45 ping et al. 2013a,b) have fueled the debate about the
46 existence and habitability of exomoons and incentivized
47 others to develop models for the surface conditions on
48 these worlds. While these studies considered illumination
49 effects from the star and the planet, as well as eclipses,
50 tidal heating (Heller 2012; Heller & Barnes 2013b,a), and
51 the transport of energy in the moon’s atmosphere (For-
52 gan & Kipping 2013), the magnetic environment of exo-
53 moons has hitherto been unexplored.

54 Moons around giant planets are subject to high-energy
55 radiation from (1) cosmic particles, (2) the stellar wind,
56 and (3) particles trapped in the planet’s magnetosphere
57 (Baumstark-Khan & Facius 2002). Contributions (1)

58 and (2) are much weaker inside the planet’s magneto-
59 sphere than outside, but effect (3) can still have detri-
60 mental consequences. The net effect (beneficial or detri-
61 mental) on a moon’s habitability depends on the actual
62 orbit, the extent of the magnetosphere, the intrinsic mag-
63 netosphere of the moon, the stellar wind, etc.

64 Stellar mass-loss and X-ray and extreme UV (XUV)
65 radiation can cause the atmosphere of a terrestrial world
66 to be stripped off. Light bodies are in particular dan-
67 ger, as their surface gravity is weak and volatiles can
68 escape easily (Lammer et al. 2013). Mars, for example,
69 is supposed to have lost vast amounts of CO₂, N, O,
70 and H (the latter two formerly bound as water) (McEl-
71 roy 1972; Pepin 1994; Vaillie et al. 2010). Intrinsic and
72 extrinsic magnetic fields can help moons sustain their at-
73 mospheres and they are mandatory to shield life on the
74 surface against galactic cosmic rays (Griessmeier et al.
75 2009). High-energy radiation can also affect the atmo-
76 spheric chemistry, thereby spoiling signatures of spectral
77 biomarkers, especially of ozone (Segura et al. 2010).

78 Understanding the evolution of the magnetic environ-
79 ments of exomoons is thus crucial to assess their habit-
80 ability. We here extend models recently applied to the
81 evolution of magnetospheres around terrestrial planets
82 under an evolving stellar wind (Zuluaga et al. 2013). Em-
83 ployed on giant planets, they allow us a first approach
84 toward parameterizing the potential of a giant planet’s
85 magnetosphere to affect potentially habitable moons.

86 2. METHODS

87 In the following, we model a range of hypothetical sys-
88 tems to explore the potential of a giant planet’s mag-

netosphere to embrace moons that are habitable from a tidal and energy budget point of view.

2.1. Bodily Characteristics of the Star

M dwarf stars are known to show strong magnetic bursts, eventually coupled with the emission of XUV radiation as well as other high-energy particles (Gurzadian 1970; Silvestri et al. 2005). Moreover, stars with masses below 0.2–0.5 solar masses (M_\odot) cannot possibly host habitable moons, since stellar perturbations excite hazardous tidal heating in the satellites (Heller 2012). We thus concentrate on stars more similar to the Sun. G dwarfs, however, are likely too bright and too massive to allow for exomoon detections in the near future. As a compromise, we choose a 0.7 M_\odot K dwarf star with solar metallicity $Z = 0.0152$ and derive its radius (R_\star) and effective temperature ($T_{\text{eff},\star}$) at an age of 100 Myr (Bressan et al. 2012): $R_\star = 0.597 R_\odot$ (R_\odot being the solar radius), $T_{\text{eff},\star} = 4270$ K. These values are nearly constant over the next couple of Gyr.

2.2. Bodily Characteristics of the Planet

We use planetary evolution models of Fortney et al. (2007) to explore two extreme scenarios, between which we expect most giant planets: (1) mostly gaseous with a core mass $M_c = 10$ Earth masses (M_\oplus) and (2) planets with comparatively massive cores. Class (1) corresponds to larger planets for given planetary mass (M_p). Models for suite (2) are constructed in the following way. For $M_p < 0.3 M_{\text{Jup}}$, we interpolate between radii of planets with core masses $M_c = 10, 25, 50$ and $100 M_\oplus$ to construct Neptune-like worlds with a total amount of 10% hydrogen (H) and helium (He) by mass. For $M_p > 0.3 M_{\text{Jup}}$, we take the precomputed $M_c = 100 M_\oplus$ grid of models. These massive-core planets (2) yield an estimate of the *minimum* radius for given M_p . To account for irradiation effects on planetary evolution, we apply the Fortney et al. (2007) models for planets at 1 AU from the Sun.

As it is desirable to compare our scaling laws for the magnetic properties of giant exoplanets with known magnetic dipole moments of solar system worlds, we start out by considering a Neptune-, a Saturn-, and a Jupiter-class host planet. For the sake of consistency, we attribute total masses of 0.05, 0.3, and $1 M_{\text{Jup}}$, as well as $M_c = 10, 25$, and again $10 M_\oplus$, respectively.

2.3. Bodily Characteristics of the Moon

Kepler has been shown capable of detecting moons as small as $0.2 M_\oplus$ combining measurements of the planet’s transit timing variation and transit duration variation (Kipping et al. 2009). The detection of a planet as small as 0.3 Earth radii (R_\oplus), almost half the radius of Mars (Barclay et al. 2013), around a K star suggests that direct transit measurements of Mars-sized moons may be possible with current or near-future technology (Sartoretti & Schneider 1999; Szabó et al. 2006; Kipping 2011). Yet, in-situ formation of satellites is restricted to a few times $10^{-4} M_p$ at most (Canup & Ward 2006; Sasaki et al. 2010; Ogihara & Ida 2012). For a Jupiter-mass planet, this estimate yields a satellite of about $0.03 M_\oplus \approx 0.3$ times the mass of Mars. Alternatively, moons can form via a range of other mechanisms (for a review, see Section 2.1 in Heller & Barnes 2013b). We therefore suspect

moons of roughly the mass and size of Mars to exist and to be detectable in the near future.

Following Fortney et al. (2007) and assuming an Earth-like rock-to-mass fraction of 68%, we derive a radius of 0.94 Mars radii or $0.5 R_\oplus$ for a Mars-mass exomoon. Tidal heating in the moon is calculated using the model of Leconte et al. (2010) and assuming an Earth-like time lag of the moon’s tidal bulge $\tau_s = 638$ s as well as a second degree tidal Love number $k_{2,s} = 0.3$ (Heller et al. 2011).

2.4. The Stellar Habitable Zone

We investigate a range of planet-moon binaries located in the center of the stellar HZ. Therefore, we compute the arithmetic mean of the inner HZ edge (given by the moist greenhouse effect) and the outer HZ edge (given by the maximum greenhouse) around a K dwarf star (Section 2.1) using the model of Kopparapu et al. (2013). For this particular star, we localize the center of the HZ at 0.56 AU.

2.5. The Runaway Greenhouse and Io Limits

The tighter a moon’s orbit around its planet, the more intense the illumination it receives from the planet and the stronger tidal heating. Ultimately, there exists a minimum circumplanetary orbital distance, at which the moon becomes uninhabitable, called the “habitable edge” (Heller & Barnes 2013b). As tidal heating depends strongly on the orbital eccentricity e_{ps} , amongst others, the radius of the HE also depends on e_{ps} .

We consider two thresholds for a transition into an uninhabitable state: (1) When the moon’s tidal heating reaches a surface flux similar to that observed on Jupiter’s moon Io, that is 2 W m^{-2} , then enhanced tectonic activity as well as hazardous volcanism may occur. Such a scenario could still allow for a substantial area of the moon to be habitable, as tidal heat leaves the surface through hot spots, (see Io and Enceladus, Ojakangas & Stevenson 1986; Spencer et al. 2006; Tobie et al. 2008), and there may still exist habitable regions on the surface. Hence, we consider this “Io-limit HE” (Io HE) as a pessimistic approach. (2) When the moon’s global energy flux exceeds the critical flux to become a runaway greenhouse (RG), then any liquid surface water reservoirs can be lost due to photodissociation into hydrogen and oxygen in the high atmosphere (Kasting 1988). Eventually, hydrogen escapes into space and the moon will be desiccated forever. We apply the semi-analytic RG model of Pierrehumbert (2010) (see Equation 1 in Heller & Barnes 2013b) to constrain the innermost circumplanetary orbit at which a moon with given eccentricity would just be habitable. For our prototype moon, this model predicts a limit of 269 W m^{-2} above which the moon would transition to an RG state. We call the corresponding critical semi-major axis the “runaway greenhouse HE” (RG HE) and consider it as an optimistic approach.

We calculate the Io and RG HEs for $e_{\text{ps}} \in \{0.1, 0.01, 0.001\}$ using Equation (22) from Heller & Barnes (2013b) and introducing two modifications. First, the planetary surface temperature (T_p) depends on the equilibrium temperature (T_p^{eq}) due to absorbed stellar light and on an additional component (T_{int}) from internal heating: $T_p = ([T_p^{\text{eq}}]^4 + T_{\text{int}}^4)^{1/4}$. Second, we use a

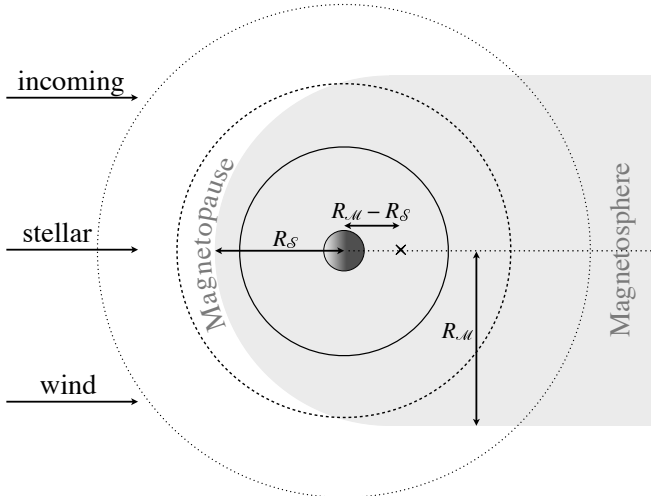


Figure 1. Sketch of the planetary magnetosphere. R_S denotes the standoff distance, R_M labels the radius of the magnetopause. A range of satellite orbits illustrates how a moon can periodically dive into and out of the planetary magnetosphere. Conceptually, the dashed orbit resembles that of Titan around Saturn, with occasional shielding and exposition to the solar wind (Bertucci et al. 2008). At orbital distances $\gtrsim 2R_S$, the fraction of the moon’s orbit spent outside the planet’s magnetospheric cavity reaches $\approx 80\%$.

Bond albedo $\alpha_{\text{opt}} = 0.3$ for the stellar illumination absorbed by the moon and $\alpha_{\text{IR}} = 0.05$ for the light absorbed from the relatively cool planet (Heller & Barnes 2013a).

2.6. Planetary Dynamos

We apply scaling laws for the magnetic field strength (Olson & Christensen 2006) that consider convection in a spherical conducting shell inside a giant planet and a convective power Q_{conv} (Equation (28) in Zuluaga et al. 2013), provided by the Fortney et al. (2007) models. The ratio between inertial forces to Coriolis forces is crucial in determining the field regime — be it dipolar- or multipolar-dominated — for the dipole field strength on the planetary surface. We scale the ratio between dipolar and total field strengths following Zuluaga & Cuartas (2012).

The core density (ρ_c) is estimated by solving a polytropic model of index 1 (Hubbard 1984). Radius and extent of the convective region are estimated by applying a semi-empirical scaling relationship for the dynamo region (Grießmeier 2006). Thermal diffusivity κ is assumed equal to 10^{-6} for all planets (Guillot 2005). Electrical conductivity σ is assumed to be 6×10^4 for planets rich in H and He, and $\sigma = 1.8 \times 10^4$ for the ice-rich giants (Olson & Christensen 2006).

We have verified that our model predicts dynamo regions that are similar to results obtained by more sophisticated analyses. For Neptune, our model predicts a dynamo radius $R_c = 0.77$ planetary radii (R_p) and $\rho_c = 3000 \text{ kg m}^{-3}$, in good agreement to Kaspi et al. (2013). We also ascertained the dynamo scaling laws to reasonably reproduce the planetary dipole moments of Ganymede, Earth, Uranus, Neptune, Saturn, and Jupiter (J. I. Zuluaga et al., in preparation). For the mass range considered here, the predicted dipole moments agree within a factor of two to six. Discrepancies of this magnitude are sufficient for our estimation of magnetospheric

properties, because they scale with $M_{\text{dip}}^{1/3}$. Significant underestimations arise for Neptune and Uranus, which have strongly non-dipolar surface fields.

2.7. Evolution of the Magnetic Standoff Distance

The shape of the planet’s magnetosphere can be approximated as a combination of a semi-sphere with radius R_M and a cylinder representing the tail region (Figure 1). The planet is at a distance $R_M - R_S$ off the sphere’s center, with

$$R_S = \left(\frac{\mu_0 f_0^2}{8\pi^2} \right)^{1/6} \mathcal{M}^{1/3} P_{\text{sw}}^{-1/6} \quad (1)$$

being the standoff distance, $\mu_0 = 4\pi \times 10^{-7} \text{ N A}^{-2}$ the vacuum magnetic permeability, $f_0 = 1.3$ a geometric factor, \mathcal{M} planetary magnetic dipole moment, and $P_{\text{sw}} \propto n_{\text{sw}} v_{\text{sw}}$ the dynamical pressure of the stellar wind. Number densities n_{sw} and velocities v_{sw} of the stellar wind are calculated using a hydrodynamical model (Parker 1958). Both quantities evolve as the star ages. Thus, we use empirical formulae (Grießmeier et al. 2007) to parameterize their time dependence.

Observations of stellar winds from young stars are challenging, and thus the models only cover stars older than 700 Myr. We extrapolate these models back to 100 Myr, although there are indications that stellar winds “saturate” when going back in time (J. Linsky 2012, private communication).

3. RESULTS

3.1. Evolution of Magnetic Standoff Distance versus Runaway Greenhouse and Io Habitable Edges

Figure 2 visualizes the evolution of R_S (thick blue line) as a snail curling around the planet, indicated by a dark circle in the center. Stellar age (t_*) is denoted in units of Gyr along the snail, starting at 0.1 Gyr at “noon” and ending after 4.6 Gyr at “midnight”. R_S , as well as the RG and Io HEs, are given in units of R_p . At $t_* = 0.1$ Gyr ($t_* = 4.6$ Gyr), $R_p = 0.385, 1.023,$ and $1.195 R_{\text{Jup}}$ (0.329, 0.862, and $1.056 R_{\text{Jup}}$) for the Neptune-, Saturn-, and Jupiter-like planets, respectively.

In panel (a) for the Neptune-like host, R_S starts very close to the planet and even inside the RG HE for the $e_{\text{ps}} = 0.001$ case (thin black snail), at roughly $2 R_p$ from the planetary center. This means, at an age of 0.1 Gyr any Mars-like satellite with $e_{\text{ps}} = 0.001$ would need to orbit beyond $2 R_p$ to avoid transition into a RG state, where it would not be affected by the planet’s magnetosphere. As the system ages, wider orbits are enshrouded by the planetary magnetic field, until after 4.6 Gyr, R_S reaches as far as the Io HE for $e_{\text{ps}} = 0.1$ (thick dashed line).¹ In summary, moons in low-eccentricity orbits around Neptune-like planets can be close the planet and be habitable from an illumination and tidal heating point of view, but it will take at least 300 Myr in our specific case until they get coated by the planet’s magnetosphere. Exomoons on more eccentric orbits will either be uninhabitable or affected by the planet’s magnetosphere after more than 300 Myr.

¹ Note that as the planet shrinks, the RG and Io HEs move outward, too. This is because of our visualization in units of planetary radii, while the values of the HEs remain constant in secular units.

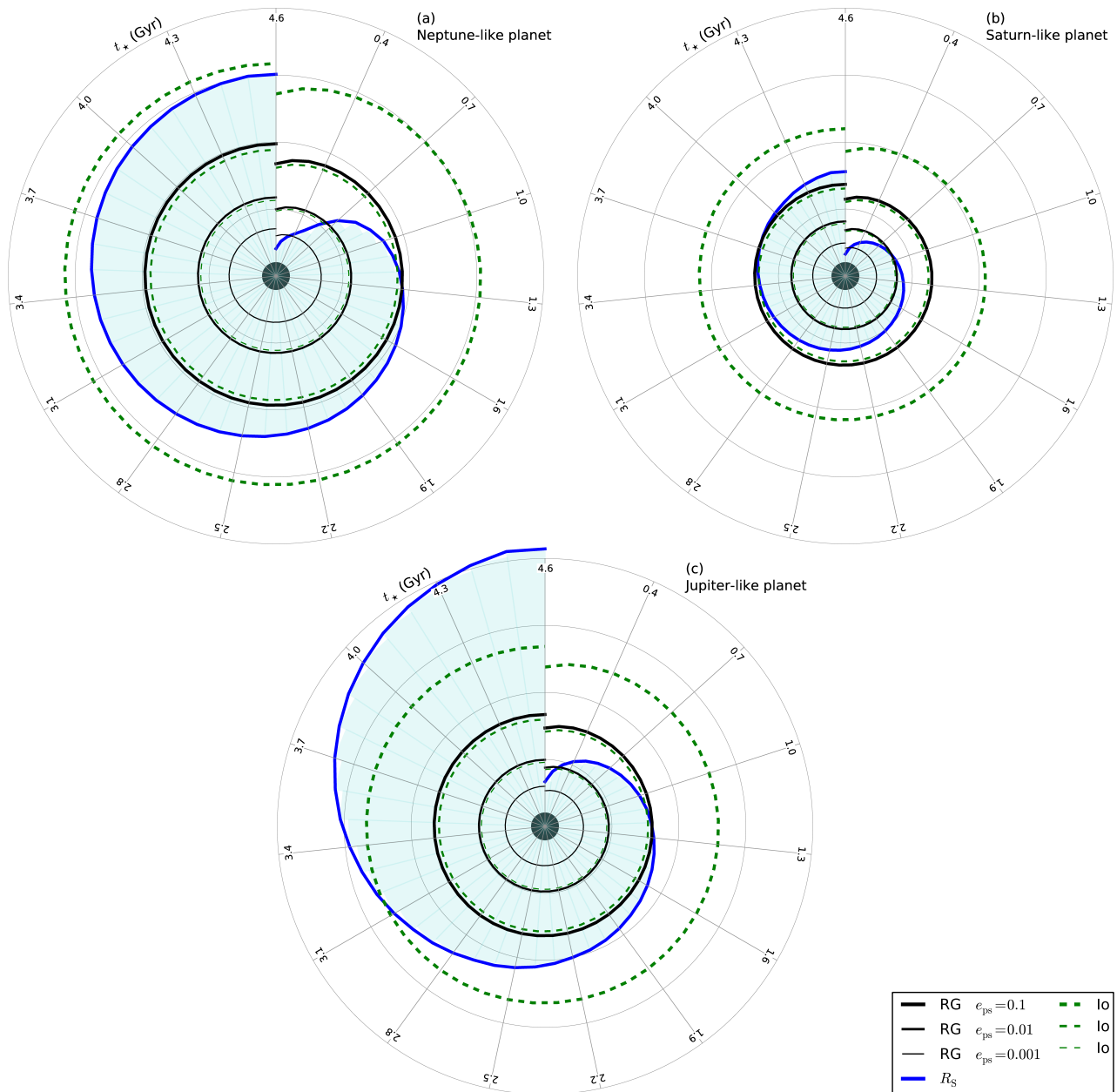


Figure 2. Evolution of the magnetic shielding (blue curves) compared to the RG HEs (solid black lines) and Io-like HEs (dashed green lines). Thick lines correspond to HEs for $e_{ps} = 0.1$, intermediate thickness to $e_{ps} = 0.01$, and thin circles to $e_{ps} = 0.001$. Thin gray lines denote distances in intervals of 5 planetary radii. The filled circle in the center symbolizes the planetary radius. Panel (a) shows a Neptune-like host, (b) a Saturn-like planet, and (c) a Jupiter-like planet. In all computations, a Mars-sized moon is assumed, and the planet-moon binary orbits a K dwarf in the center of the stellar HZ.

301 Moving on to Figure 2(b) and the Saturn-like host, 314
 302 we find that R_S reaches the $e_{ps} = 0.001$ RG HE after 315
 303 roughly 200 Myr, but it transitions all the other HEs 316
 304 substantially later than in the case of a Neptune-like host. 317
 305 After ≈ 1 Gyr, the $e_{ps} = 0.01$ RG HE and the Io HE for 318
 306 $e_{ps} = 0.01$ are transversed. After 4.6 Gyr, all orbits ex- 319
 307 cept for the Io HE at an eccentricity of 0.1 are covered by 320
 308 the planet’s magnetic field. In conclusion, close-in Mars- 321
 309 sized moons around Saturn-like planets can be magneti- 322
 310 cally affected early on and be habitable from a RG or 323
 311 tidal heating point of view, if their orbital eccentricities 324
 312 are small.

313 Finally, Figure 2(c) shows that exomoons at the RG 325

HE of Jovian planets for $e_{ps} = 0.001$ will be bathed in
 the planetary magnetosphere at stellar ages as young as
 100 Myr. After roughly 1.3 Gyr, R_S transitions the RG
 HE for $e_{ps} = 0.1$ and the Io HE for $e_{ps} = 0.01$. Even
 the Io HE with an eccentricity of $e_{ps} = 0.1$ is covered
 at around 3.1 Gyr. After 4.6 Gyr, the planet’s magnetic
 shield reaches as far as $21 R_p$. Clearly, exomoons about
 Jupiter-like planets face the greatest prospects of inter-
 ference with the planetary magnetosphere, even in orbits
 that are sufficiently wide to ensure negligible tidal heat-
 ing.

3.2. Minimum Magnetic Dipole Moment

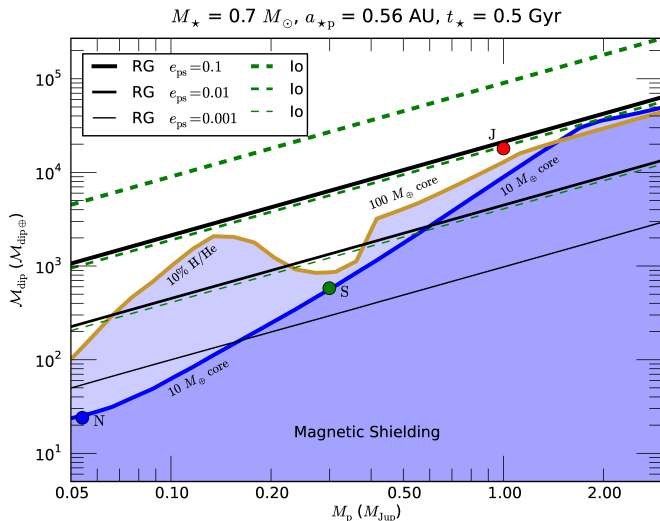


Figure 3. Magnetic dipole moments (ordinate) for a range of planetary masses (abscissa). The straight lines depict M_{dip} as it would be required at an age of 0.5 Gyr in order to shield a moon at a given HE (solid: runaway greenhouse; dashed: Io-like heating). Low-mass giants obviously fail to protect their moons beyond most HEs, while Jupiter-like planets offer a range of shielded orbits beyond the RG and Io HEs. Neptune, Saturn, and Jupiter are indicated with filled circles.

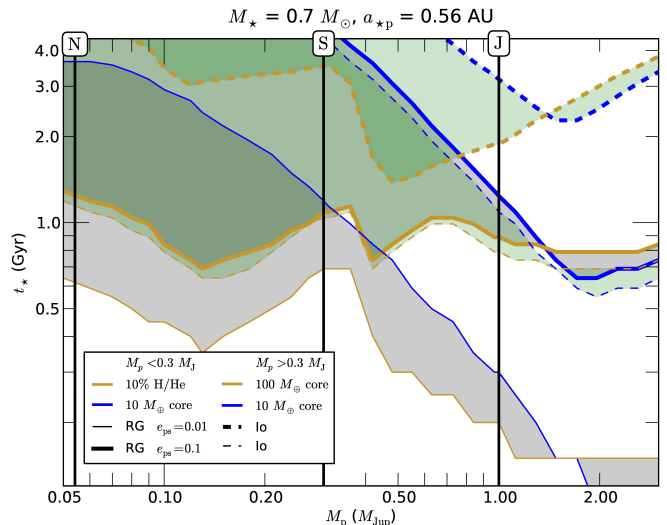


Figure 4. Time required by the planet’s magnetic standoff radius R_S to envelop the Io (dashed) and RG (solid) HEs. Shaded regions illustrate uncertainties coming from planetary structure models, with the boundaries corresponding to a high- and a low-core mass planetary model, respectively (brown and blue lines). In general, the magnetic standoff distance around more massive planets requires less time to enshroud moons at a given HE.

Looking at the standoff radii for the three cases in Figure 2, we wonder how strong the magnetic dipole moment M_{dip} would need to be after 0.5 Gyr, when the atmospheric buildup should have mostly ceased, in order to magnetically enwrap the moon at a given HE. This question is answered in Figure 3.

While planets with relatively massive cores (brown solid line) shield a wider range of orbits for given M_p below roughly $1M_{\text{Jup}}$, the low-mass core model (blue solid line) catches up for more massive giants. What is more, our model tracks for the predicted M_{dip} , which we expect to be located between the thick brown and thick blue line, “overtake” the RG and Io-like HEs for a range of eccentricities. HE contours that fall within the shaded area, are magnetically protected, while moons above a certain HE are habitable from a tidal and illumination point of view.

We finally examine temporal aspects of magnetic shielding in Figure 4. The question answered in this plot is: “How long would it take a planet to magnetically coat its moon beyond the habitable edges?”. Again, planetary mass is along the abscissa, but now stellar life time t_* is along the ordinate. Clearly, the magnetic standoff radius of lower-mass planets requires more time to expand out to the respective HEs. While low-mass giants with low-mass cores (blue lines) require up to 3.5 Gyr to reach the RG HE for $e_{\text{ps}} = 0.01$, equally mass planets but with a high-mass core (thin brown line) could require as few as 650 Myr.

Planets more massive than roughly $0.3 M_{\text{Jup}}$, will coat their moons at the RG HE for $e_{\text{ps}} = 0.01$ as early as 1 Gyr after formation. For lower eccentricities, time scales decrease. As the RG HE is more inward to the planet than the Io HE, it is coated earlier than the Io limit for given e_{ps} . RG and Io HEs for $e_{\text{ps}} = 0.001$ are not shown as they are covered earlier than ≈ 300 Myr in all cases.

4. CONCLUSION

Mars-sized exomoons of Neptune-sized exoplanets in the stellar HZ of K stars will hardly be affected by planetary magnetospheres if these moons are habitable from an illumination and tidal heating point of view. While the magnetic standoff distance expands for higher-mass planets, ultimately Jovian hosts can enshroud their massive moons beyond the HE, depending on orbital eccentricity. In any case, exomoons beyond about $20 R_p$ will be habitable in terms of illumination and tidal heating, and they will not be coated by the planetary magnetosphere within about 4.5 Gyr. Moons between 5 and $20 R_p$ can be habitable, depending on orbital eccentricity, and be affected by the planetary magnetosphere at the same time.

Uncertainties in the parameterization of tidal heating cause uncertainties in the extent of both the RG and Io HEs. Once a potentially habitable exomoon would be discovered, detailed interior models for the satellite’s behavior under tidal stresses would need to be explored.

In a forthcoming study, we will examine the evolution of planetary dipole fields, and we will apply our methods to planets and candidates from the *Kepler* sample. Obviously, a range of giant planets resides in their stellar HZs, and these planets need to be prioritized for follow-up search on the potential of their moons to be habitable.

The referee report of Jonathan Fortney substantially improved the quality of this study. We have made use of NASA’s ADS Bibliographic Services. Computations have been performed with *ipython* 0.13 on *python* 2.7.2 (Pérez & Granger 2007). RH receives funding from the Canadian Astrobiology Training Program. JIZ is supported by CODI-UdeA and Colciencias.

REFERENCES

- Barclay, T., Rowe, J. F., Lissauer, J. J., et al. 2013, *Nature*, 494, 452
 Batalha, N. M., Rowe, J. F., Bryson, S. T., et al. 2013, *ApJS*, 204, 24

- 399 Baumstark-Khan, C., & Facius, R. 2002, Life under conditions of
400 ionizing radiation, ed. G. Horneck & C. Baumstark-Khan
401 (Springer Verlag, Berlin Heidelberg New York), 261–284
402 Bertucci, C., Achilleos, N., Dougherty, M. K., et al. 2008, *Science*,
403 321, 1475
404 Borucki, W. J., Koch, D., Basri, G., et al. 2010, *Science*, 327, 977
405 Bressan, A., Marigo, P., Girardi, L., et al. 2012, *MNRAS*, 427, 127
406 Canup, R. M., & Ward, W. R. 2006, *Nature*, 441, 834
407 Forgan, D., & Kipping, D. 2013, *MNRAS*, 432, 2994
408 Fortney, J. J., Marley, M. S., & Barnes, J. W. 2007, *ApJ*, 659,
409 1661
410 Grießmeier, J.-M. 2006, PhD thesis, Technische Universität
411 Braunschweig
412 Grießmeier, J.-M., Preusse, S., Khodachenko, M., et al. 2007,
413 *Planet. Space Sci.*, 55, 618
414 Grießmeier, J.-M., Stadelmann, A., Grenfell, J. L., Lammer, H.,
415 & Motschmann, U. 2009, *Icarus*, 199, 526
416 Guillot, T. 2005, *Annual Review of Earth and Planetary Sciences*,
417 33, 493
418 Gurzadian, G. A. 1970, *Boletín de los Observatorios Tonantzintla*
419 *y Tacubaya*, 5, 263
420 Heller, R. 2012, *A&A*, 545, L8
421 Heller, R., & Barnes, R. 2013a, *International Journal of*
422 *Astrobiology*, (submitted)
423 —. 2013b, *Astrobiology*, 13, 18
424 Heller, R., Leconte, J., & Barnes, R. 2011, *A&A*, 528, A27
425 Hubbard, W. B. 1984, New York, Van Nostrand Reinhold Co.,
426 1984, 343 p., 1
427 Kaltenegger, L., & Sasselov, D. 2011, *ApJ*, 736, L25
428 Kaspi, Y., Showman, A. P., Hubbard, W. B., Aharonson, O., &
429 Helled, R. 2013, *Nature*, 497, 344
430 Kasting, J. F. 1988, *Icarus*, 74, 472
431 Kasting, J. F., Whitmire, D. P., & Reynolds, R. T. 1993, *Icarus*,
432 101, 108
433 Kipping, D. M. 2011, *MNRAS*, 416, 689
434 Kipping, D. M., Forgan, D., Hartman, J., et al. 2013a, *ArXiv*
435 e-prints
436 Kipping, D. M., Fossey, S. J., & Campanella, G. 2009, *MNRAS*,
437 400, 398
438 Kipping, D. M., Hartman, J., Buchhave, L. A., et al. 2013b, *ApJ*,
439 770, 101
440 Kopparapu, R. K., Ramirez, R., Kasting, J. F., et al. 2013, *ApJ*,
441 765, 131
442 Lammer, H., Kislyakova, K. G., Güdel, M., et al. 2013, in *The*
443 *Early Evolution of the Atmospheres of Terrestrial Planets*
444 (Springer, New York), 33–52
445 Leconte, J., Chabrier, G., Baraffe, I., & Levrard, B. 2010, *A&A*,
446 516, A64
447 McElroy, M. B. 1972, *Science*, 175, 443
448 Ogihara, M., & Ida, S. 2012, *ApJ*, 753, 60
449 Ojakangas, G. W., & Stevenson, D. J. 1986, *Icarus*, 66, 341
450 Olson, P., & Christensen, U. R. 2006, *Earth and Planetary*
451 *Science Letters*, 250, 561
452 Parker, E. N. 1958, *ApJ*, 128, 664
453 Pepin, R. O. 1994, *Icarus*, 111, 289
454 Pérez, F., & Granger, B. E. 2007, *Comput. Sci. Eng.*, 9, 21
455 Pierrehumbert, R. T. 2010, *Principles of Planetary Climate*
456 (Cambridge University Press, New York)
457 Reynolds, R. T., McKay, C. P., & Kasting, J. F. 1987, *Advances*
458 *in Space Research*, 7, 125
459 Sartoretti, P., & Schneider, J. 1999, *A&AS*, 134, 553
460 Sasaki, T., Stewart, G. R., & Ida, S. 2010, *ApJ*, 714, 1052
461 Segura, A., Walkowicz, L. M., Meadows, V., Kasting, J., &
462 Hawley, S. 2010, *Astrobiology*, 10, 751
463 Silvestri, N. M., Hawley, S. L., & Oswald, T. D. 2005, *AJ*, 129,
464 2428
465 Spencer, J. R., Pearl, J. C., Segura, M., et al. 2006, *Science*, 311,
466 1401
467 Szabó, G. M., Szatmáry, K., Divéki, Z., & Simon, A. 2006, *A&A*,
468 450, 395
469 Tobie, G., Čadež, O., & Sotin, C. 2008, *Icarus*, 196, 642
470 Valeille, A., Bougher, S. W., Tennishev, V., Combi, M. R., &
471 Nagy, A. F. 2010, *Icarus*, 206, 28
472 Williams, D. M., Kasting, J. F., & Wade, R. A. 1997, *Nature*,
473 385, 234
474 Zuluaga, J. I., Bustamante, S., Cuartas, P. A., & Hoyos, J. H.
475 2013, *ApJ*, 770, 23
476 Zuluaga, J. I., & Cuartas, P. A. 2012, *Icarus*, 217, 88